Journal of Alloys and Compounds 509 (2011) L267–L272

Contents lists available at ScienceDirect

Journal of Alloys and Compounds

journal homepage: www.elsevier.com/locate/jallcom

Letter

A mild biomolecule-assisted route for preparation of flower-like $AgBiS_2$ crystals

Haitao Liu[a], Jiasong Zhong[b], Xiaojuan Liang[a], Jingfeng Zhang[a], Weidong Xiang[a,b,*]

[a] College of Chemistry and Materials Engineering, Wenzhou University, Wenzhou 325035, China
[b] College of Materials Science and Engineering, Tongji University, Shanghai 200092, China

ARTICLE INFO

Article history:
Received 29 August 2010
Received in revised form 7 April 2011
Accepted 9 April 2011
Available online 20 April 2011

Keywords:
$AgBiS_2$
L-cystine
Semiconductor
Ternary chalcogenide
Chemical synthesis

ABSTRACT

A mild biomolecule-assisted route for preparation of flower-like $AgBiS_2$ crystals was developed via reactions among $AgNO_3$, $BiCl_3$, and L-cystine in *N,N*-dimethylformamide (DMF) at 200 °C for 12 h. L-cystine was used as both the sulfide source and complexing agent. The as-synthesized $AgBiS_2$ crystals were characterized by XRD, EDS, XPS, PL, FESEM, TEM, HRTEM, and SAED. Results showed that the synthesized $AgBiS_2$ crystals had stoichiometric composition, good crystallinity, and flower-like morphology. A possible formation mechanism for flower-like $AgBiS_2$ crystals was also discussed based on the experiment.

© 2011 Elsevier B.V. All rights reserved.

1. Introduction

In recent years, I–V–VI ternary chalcogenide semiconducting compounds have driven extensive research interest because of their potential and practical applications in linear, nonlinear, optoelectronic, and thermoelectric devices, as well as optical recording media [1–5]. $AgBiS_2$, one of the important I–V–VI ternary semiconductors, has promising applications as a novel mineral semiconductor due to its unusual electronic and magnetic properties [6–8]. It has high potential to use as optoelectric and thermoelectric devices including optical recording media [7,8]. Traditionally, $AgBiS_2$ is prepared by direct combination of the elements (silver, bismuth, and sulfur) or by thermal annealing of mixtures of binary sulfides [9]. Recently, using softer chemical approach to $AgBiS_2$ synthesis has been paid considerable attention because of their particular advantages in the synthesis of the various kinds of shape crystals [10]. To the best of our knowledge, few reports on the synthesis of $AgBiS_2$ with different morphologies have been published. Typically, dendritic $AgBiS_2$ crystals are synthesized under microwave irradiation [6]. In previous studies, nanorods and coral-shaped $AgBiS_2$ crystals were prepared by a polyol route [8,11]. The flower and hexapod $AgBiS_2$ crystals were obtained by cyclic microwave-assisted synthesis [12]. The flowers and nanowhiskers were studied via solvothermal methods [13,14], and 3D arrays of close-packed $AgBiS_2$ crystals were synthesized by sonochemical approach [15]. Although various approaches have been demonstrated in producing $AgBiS_2$ with multifarious morphologies, green synthesis is highly desirable because environmentally benign approaches may be considered relatively green chemical alternatives of practical significance [16].

Recently, biomolecule-assisted synthesis has been a promising approach to the preparation of various novel nanomaterials because biomolecules, as the basic building blocks of life, have special structures, fascinating self-assembling functions, and important technological applications, thereby serving as templates for the design and synthesis of complicated structures [17–22]. The manner by which the special structures and strong assembling functions of biomolecules are used to fabricate nanomaterials with desired shapes and complicated superstructures is very important in all of biology, chemistry, and materials science [23]. Lately, L-cystine ($C_6H_{12}N_2O_4S_2$), a small biomolecule, has been reported as both a sulfur source and a complexation in the formation of Ag_3SbS_3 and Cu_3SbS_3 nanostructures [24,25]. L-cystine is an inexpensive, simple, and environment-friendly thiol-containing amino acid, which has been extensively applied in medicine, foodstuff, cosmetic, etc. [24,25]. Thus, it would be interesting to develop a simple L-cystine-assisted approach to prepare other ternary chalcogenide semiconductor nanostructures.

In this paper, we first developed a simple and efficient route for the preparation of flower-like $AgBiS_2$ crystals via biomolecule-assisted solvothermal method.

* Corresponding author at: College of Chemistry and Materials Engineering, Wenzhou University, Wenzhou 325035, China. Tel.: +86 577 86596013; fax: +86 577 86689644.
E-mail address: weidongxiang@yahoo.com.cn (W. Xiang).

0925-8388/$ – see front matter © 2011 Elsevier B.V. All rights reserved.
doi:10.1016/j.jallcom.2011.04.073

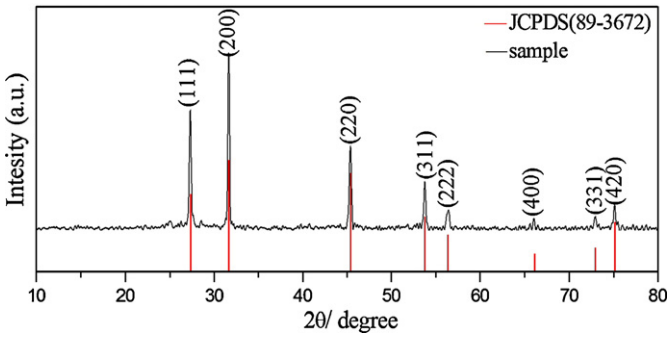

Fig. 1. Typical XRD pattern of as-prepared $AgBiS_2$ synthesized at 200 °C for 12 h.

2. Experimental

2.1. Synthesis of $AgBiS_2$ crystals

All reagents were of analytical grade and used without any further treatment. In a typical synthesis, 1 mmol $AgNO_3$, 1 mmol $BiCl_3$ and 2 mmol L-cystine were dissolved in 40 mL *N,N*-dimethylformamide (DMF) under constant stirring. Then, the obtained solution was transferred into a Teflon-lined stainless-steel autoclave with a capacity of 50 mL. The autoclave was sealed and maintained at 200 °C for 12 h. After the reaction was completed, the resultant black precipitate was filtered and washed several times with de-ionized water and absolute ethanol, and then dried in a vacuum at 55 °C for 4 h.

2.2. Characterization

The as-obtained samples were characterized by powder X-ray diffraction (XRD) on a Bruker D8-Advance X-ray diffractometer with graphite monochromated Cu Kα radiation (λ = 1.5406 Å). A scan rate of 0.02°/s was applied to record the pattern in the 2θ angular range of 10–80°. The accelerating voltage and the applied current were 40 kV and 40 mA, respectively. X-ray photoelectron spectroscopy (XPS) was performed on an ESCALAB 250 spectrometer, using Al Kα X-rays as the excitation source. The morphology of the samples was studied by field-emission scanning electron microscope (FESEM) on a JEOL instrument (JEOL-6700F) at an accelerating voltage of 10 kV. Energy dispersive spectrometry (EDS) analysis of the products was carried out on an OXFORD INCA instrument attached to the scanning electron microscope at a scanning range of 0–20 kV to determine the chemical composition. The transmission electron microscopy (TEM), high-resolution TEM (HRTEM), and selected area electron diffraction (SAED) images were recorded on an FEI Tecnai F-20 transmission electron microscope at an accelerating voltage of 200 kV. The specimens of TEM and HRTEM measurements were prepared by spreading a droplet of ethanol suspension onto a copper grid, coated with a thin layer of amorphous carbon film, and allowed to dry in air. All the measurements were carried out at room temperature. The photoluminescence (PL) spectrum was measured at room temperature on a FLuoromax-4 spectrofluorometer (HORIBA Jobin Yvon, Inc.) equipped with a 150 W xenon lamp as the excitation source.

3. Results and discussion

The phase purity of the resultant sample was examined by XRD. Fig. 1 shows that the products obtained are cubic phase $AgBiS_2$. The peaks correspond to (1 1 1), (2 0 0), (2 2 0), (3 1 1), (2 2 2), (4 0 0), (3 3 1) and (4 2 0), which are in good agreement with reported values (JCPDS No. 89-3672). No characteristic peaks of other impurities such as Ag_2S or Bi_2S_3 are observed, which confirmed that the as-obtained product is composed of pure $AgBiS_2$ crystals. The strong and sharp peaks indicated that the as-obtained $AgBiS_2$ is well crystallized.

The morphology and size of the as-obtained products were characterized by FESEM. Low-magnification images (Fig. 2(a) and (b)) show that the product is composed of large quantities of flower-like crystals with an average diameter of about 5 μm. The high-magnification image Fig. 2(c) shows that the flower-like crystals consist of a large number of petals, with thicknesses ranging from 100 to 150 nm. The chemical composition of the as-obtained flower-like $AgBiS_2$ was further determined by EDS. Only the peaks of the elements Ag, Bi, and S are present in the EDS spectrum, and the molar ratio of Ag, Bi, and S is 1:1.006:2.043, consistent with $AgBiS_2$.

The purity and composition of the product were characterized by XPS. The XPS spectra of the flower-like $AgBiS_2$ are shown in Fig. 3, which depicts the XPS survey spectra of the as-obtained products. The Ag3d core-level spectrum showed that the binding energy for $Ag3d_{5/2}$ and $Ag3d_{3/2}$ are located at 367.86 and 373.77 eV, which is close to reported values [26]. The two strong peaks at 158.09 and 163.35 eV Fig. 3(c) are attributed to $Bi4f_{7/2}$ and $Bi\ 4f_{5/2}$, which is similar in the reference [27,28]. The S 2s core-level spectrum Fig. 3(d) showed a peak located at 225.06 eV [29]. No obvious impurities could be detected in the sample, indicating that the level of impurities is lower than the resolution limit of XPS (1 at.%). The atomic ratio of Ag/Bi/S is approximately 1:1:2 according to the quantification of the peak areas of Ag3d, Bi 4f, and S2s. This result is consistent with those of XRD and EDS analyses.

The morphology and structure of the as-obtained products were further detected by TEM, HRTEM, and SAED. The as-obtained products with flower-like morphologies are clearly observable in the lower-magnification TEM image (Fig. 4(a)). Furthermore, the flower-like pattern containing petal structures is observable through the higher-magnification TEM image (Fig. 4(b)), which is also observable in FESEM analysis. Fig. 4(c) represents the SAED pattern of the as-obtained products. A number of bright spots are arranged in concentric circles, and these circles are diffuse and hollow, which indicated that the product is a poly-crystal. These diffraction circles can be resolved into four distinct planar systems with identical planar spacings, which are attributed to (1 1 1), (2 0 0), (2 2 0), and (3 1 1) crystal planes of the cubic structure. The HRTEM image of as-obtained products showed that the distance between the adjacent lattice fringes is 0.282 nm (Fig. 4(d)), which matches the spacing distance of (2 0 0) planes of the $AgBiS_2$ crystal [d(2 0 0) = 0.2824 nm].

FESEM and XRD were again employed to elucidate the growth process of the as-obtained products in different reaction stages. Fig. 5 represents the FESEM images of the as-obtained products at the different reaction times including 4, 12, and 24 h. The morphologies of these intermediates are similar at 12 h, as shown in Fig. 5(c). Meanwhile, the evolution of the as-obtained products was also characterized by XRD. As seen in Fig. 5(d), the peak positions and relative intensities of the X-ray diffraction peaks match well with the matildite $AgBiS_2$ crystalline phase (JCPDS No. 89-3672). In addition, no $AgBiS_2$ phase is obtained (data not shown) even at 160 °C for 48 h. With a reaction temperature of up to 200 °C, large quantities of $AgBiS_2$ flower-like crystals consisting of numerous nanoplates are obtained at the reaction time of 4 h (Fig. 5(a)). When the reaction time is 8 h, the resultant product in Fig. 5(b) consists of a substantial quantity of rod-like structures, as well as minimal quantities of plate-like flower-like structures. When the reaction time is prolonged to 12 h, only flower-like patterns consisting of numerous quantities of uniform petals with rod-like structures are obtained, as shown in Fig. 2(a)–(c). When the reaction time is prolonged to 24 h, $AgBiS_2$ flower-like structures are also obtained. However, the petals become larger and some are in aggregated states Fig. 5(c). According to the analysis above, we can conclude that extending the reaction time beyond 12 h is unfavorable for the formation of uniform flower-like structures.

Although the exact mechanism for L-cystine-assisted formation of flower-like $AgBiS_2$ crystals is still under investigation, the coordination interaction between Ag^+, Bi^{3+} and L-cystine is undoubtedly significant. According to previous reports, bismuth ions [30] and silver ions [31] can react with amino acids with amino- and thiol-groups to form complexes [23]. The functional groups, such as $–NH_2$, –COOH, and –S–, in the L-cystine molecule have a strong tendency to interact with inorganic cations, which was confirmed by Burford et al. via mass spectrometry [32]. When mixing the

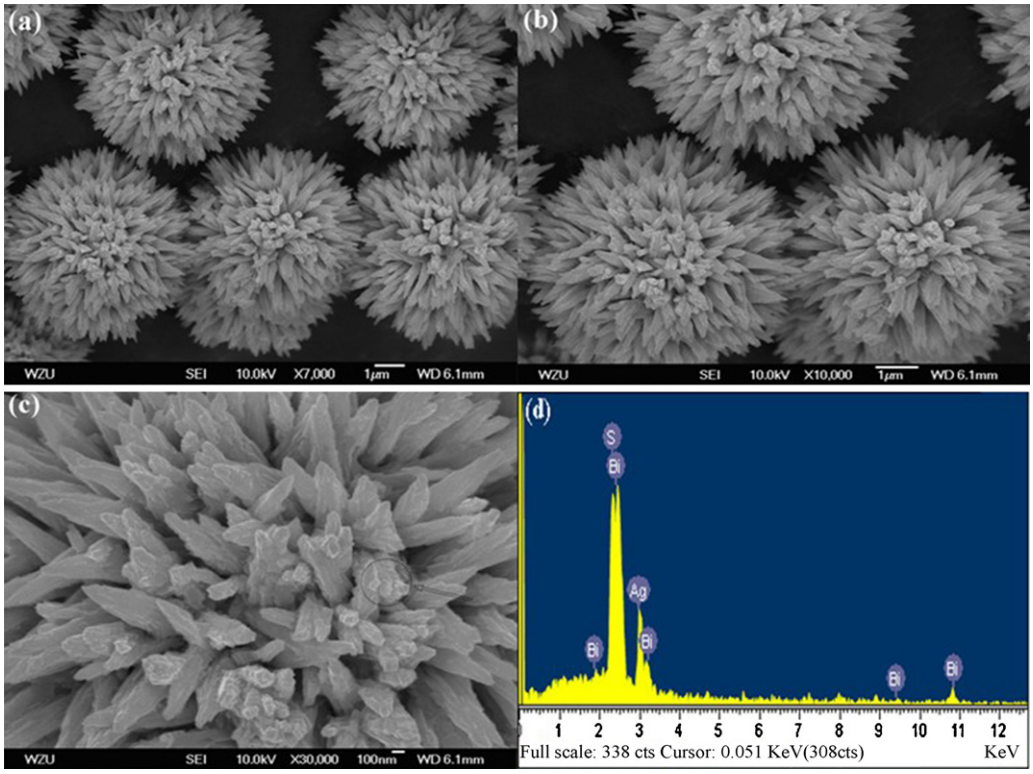

Fig. 2. Representative FESEM images of as-prepared $AgBiS_2$ products: (a) and (b) at low magnification; (c) at high magnification; (d) EDS spectrum of a single petal.

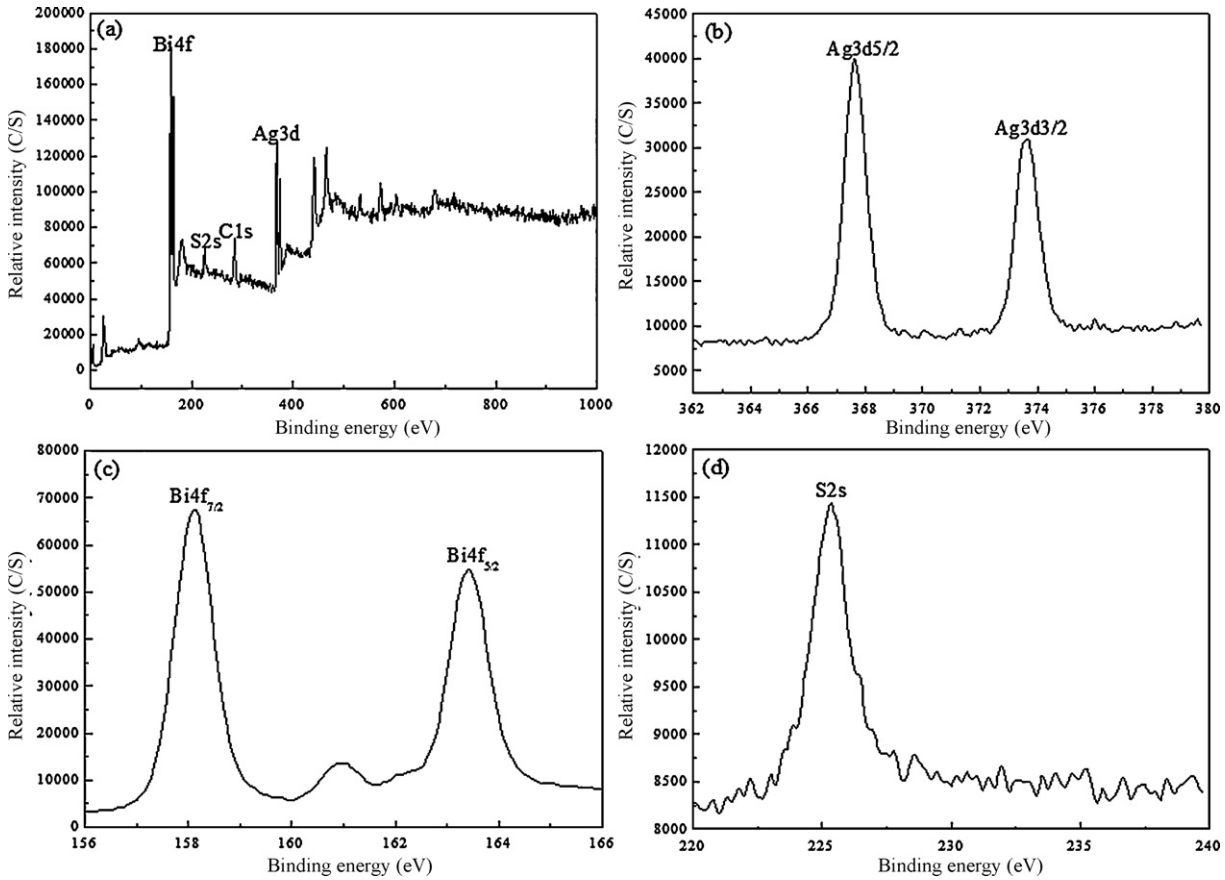

Fig. 3. XPS spectra of the $AgBiS_2$ product: (a) typical XPS survey spectrum of the $AgBiS_2$ product, (b) core level spectrum for Ag3d, (c) core level spectrum for Bi4f, and (d) core level spectrum for S2s.

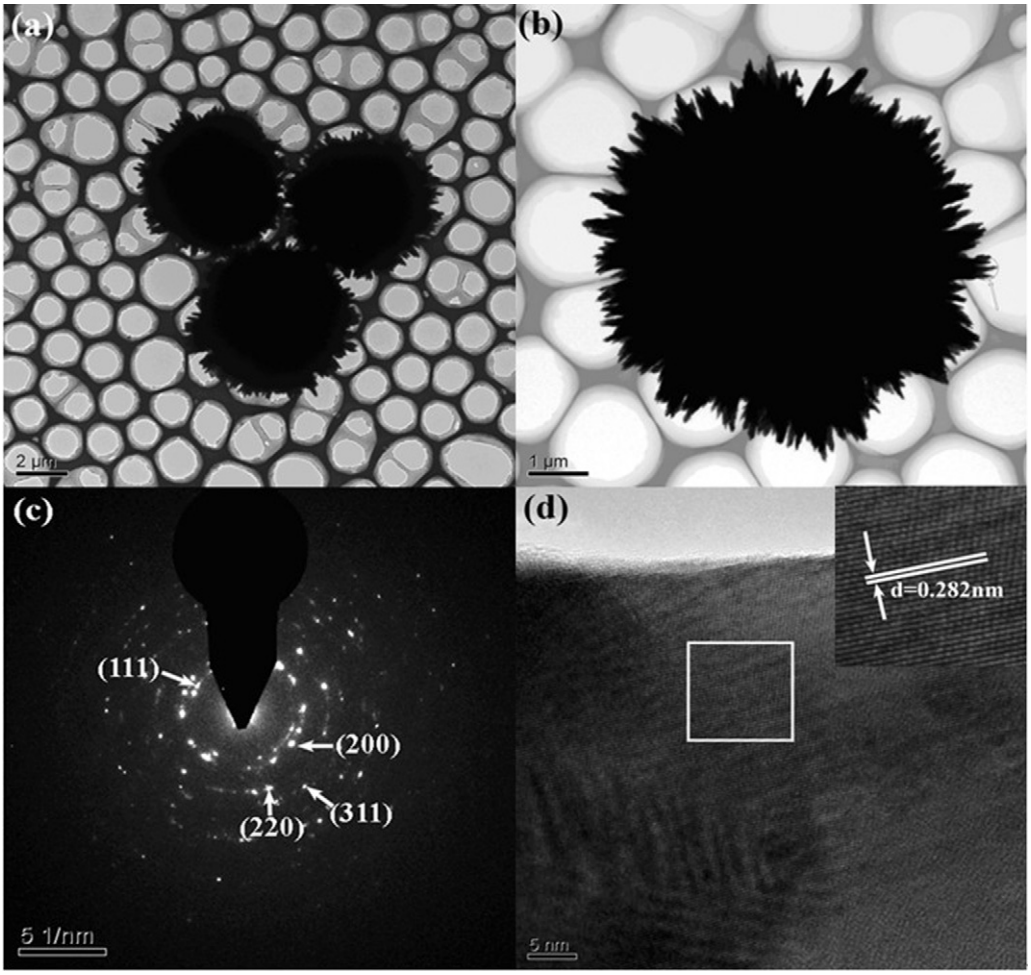

Fig. 4. (a) and (b) TEM images of $AgBiS_2$ product; (c) SAED image of the individual petal in the flowerlike; (d) the corresponding HRTEM pattern of the $AgBiS_2$ product. Inset is the distances between the adjacent lattice fringes (area marked with a rectangle).

L-cystine solution and the $Ag(NO_3)_2$ and $BiCl_3$ solutions, Ag^+, Bi^{3+} can interact with L-cystine molecules at room temperature to form precursor complexes $[Ag(\text{L-cystine})_n]^+$ and $[Bi(\text{L-cystine})_n]^{3+}$. Upon heating, L-cystine is attacked by the strong nucleophilic O atoms of H_2O molecules [33,34], which comes from the analytical DMF and hydrated metal salts, leading to the weakening of $[Ag(\text{L-cystine})_n]^+$ and $[Bi(\text{L-cystine})_n]^{3+}$ complex, which will be probably broken to release S^{2-} anion slowly. The newly formed S^{2-} then reacts with Ag^+ and Bi^{3+} to produce $AgBiS_2$ nuclei. The $(AgBiS_2)_n$ nuclei are produced, which serve as the seeds for the subsequent growth of $AgBiS_2$ crystals. Then, the freshly formed $(AgBiS_2)_n$ nuclei in the solution are unstable and numerous dangling bonds, defects, or traps are observed on the nuclei surface [35]. The $(AgBiS_2)_n$ nuclei for random moving in the solution preferentially accumulate with one another because of the acting force, and transform into $AgBiS_2$ microcrystals that were detected by XRD analysis. Nanostructured $AgBiS_2$ crystals are produced because of the influence of the orientation growth of $(AgBiS_2)_n$ nuclei. The flower-like $AgBiS_2$ crystals are obtained by the anisotropic growth in the process.

In order to discuss the influence of the synthesis on the environment, we researched further the byproduct in the reaction. Before and after the reaction, Liquid Chromatography-tandem Mass Spectrometry (SHIMADZU, GCMS-QP2010PLUS) was used to contrast the change of DMF, which indicates that DMF is not decomposed at 200 °C. Chemical analysis was used to investigate the change of L-cystine in the reaction. NH_4^+ is found in the byproduct, which indicates that N–C bond ruptures. No C–S–S spectrum band was found in the byproduct by the FT-Raman spectroscopic analysis, which indicates that C–S–S bond ruptures. So, we can conclude that the amino group ($-NH_2$) and disulfide bridge group (S–S) are removed from L-cystine molecule in the reaction at 200 °C for 12 h. Possible reactions taking place in the system can be described as follows:

$$Ag^+ + n\text{L-cystine} \xrightarrow{\text{coordination}} [Ag(\text{L-cystine})_n]^+ \quad (1)$$

$$Bi^{3+} + n\text{L-cystine} \xrightarrow{\text{coordination}} [Bi(\text{L-cystine})_n]^{3+} \quad (2)$$

$$[Ag(\text{L-cystine})_n]^+ + [Bi(\text{L-cystine})_n]^{3+} \xrightarrow{\text{decomposition}} S^{2-} + CH_3COCOO^- + NH_4^+ + Bi^{3+} + Ag^+ \quad (3)$$

$$Ag^+ + Bi^{3+} + S^{2-} \xrightarrow{\text{sulfidation}} AgBiS_2(\text{nuclei}) \quad (4)$$

Although the mechanism for the formation of $AgBiS_2$ crystals with flower-like morphology has been proposed above, its exact mechanism remains difficult to understand because the L-cystine-assisted ternary solvothermal reaction system is quite complicated and further investigation is needed.

To conduct further research on the effect of L-cystine in the synthesis of flower-like $AgBiS_2$ crystals, other sulfur sources (thiosalicylic acid, Na_2S) instead of L-cystine were used in the system at 200 °C for 12 h solvothermal reaction. The FESEM images and corresponding XRD patterns of the as-synthesized crystals are shown

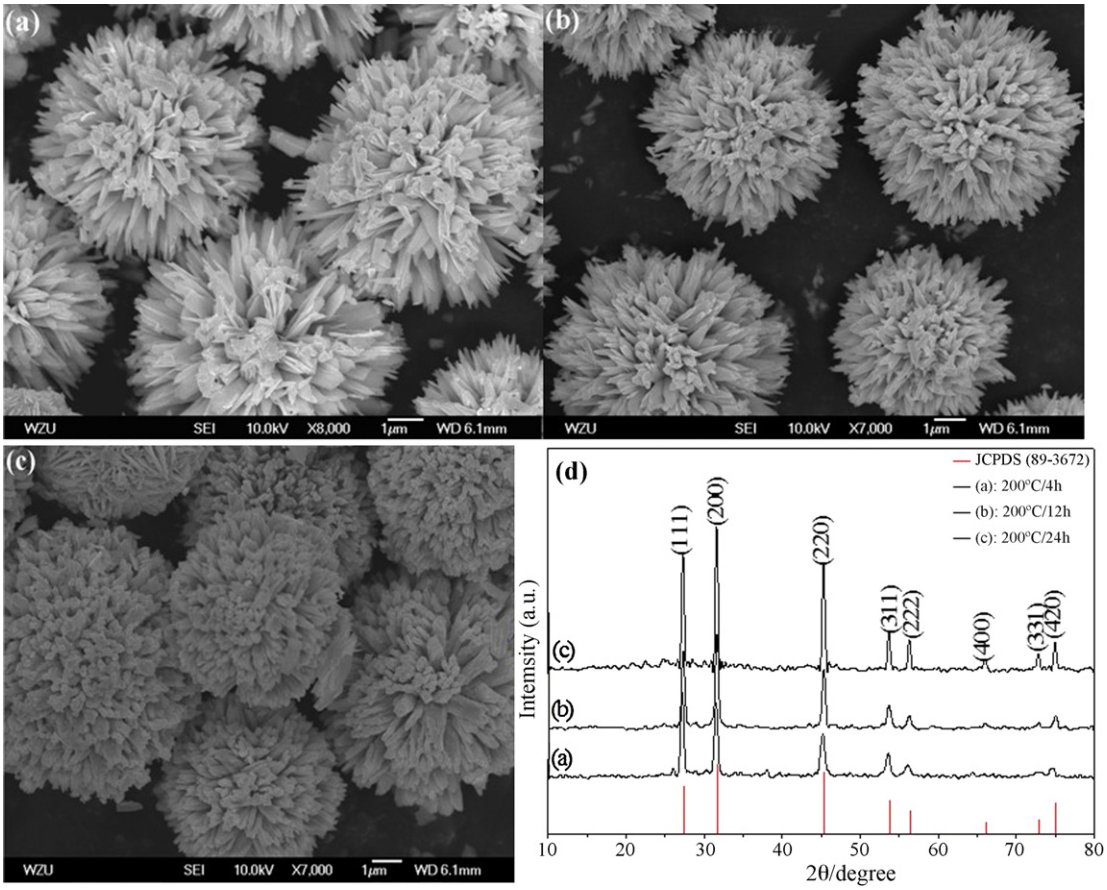

Fig. 5. Typical FESEM images of $AgBiS_2$ samples with different reaction times: (a) 4 h; (b)8 h; (c) 24 h. (d) Corresponding XRD spectra of the products produced at 200 °C.

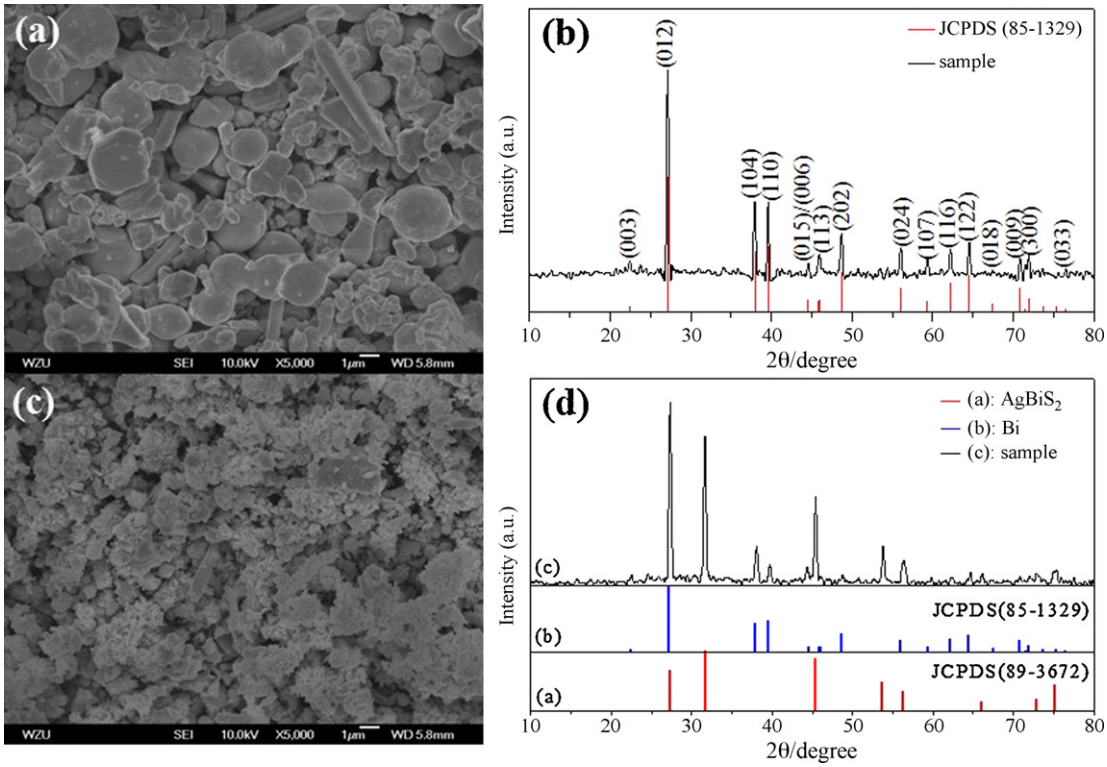

Fig. 6. The FESEM images and corresponding XRD patterns of different sulfur sources at 200 °C 12 h in DMF: (a) and (b) thiosalicylic acid; (c) and (d) Cysteine.

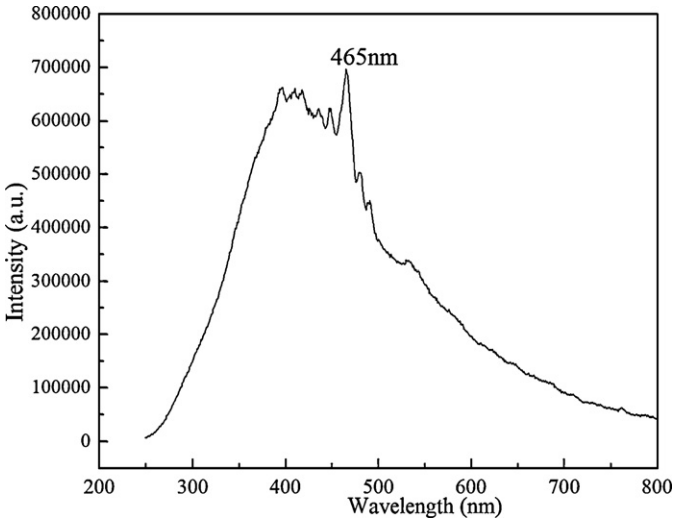

Fig. 7. PL emission spectrum of as-prepared $AgBiS_2$ synthesized at 200 °C for 12 h.

in Fig. 6(a)–(d). When the solvothermal reactions were conducted using thiosalicylic acid as the sulfur sources (with all other conditions keep constant), only Bi is obtained instead of flower-like $AgBiS_2$ crystals. Fig. 6(a) and (b) shows the typical overall FESEM image and XRD patterns of the products. FESEM image shows that the samples are consist of irregular spheres and rods [Fig. 6(a)]. All the peaks in the XRD pattern can be readily indexed to a pure hexagonal phase of Bi, which are in good agreement with the reported values (JCPDS card No. 85-1329). When we use Na_2S as the sulfur source while other conditions remain unchanged (compared with the condition of Fig. 2), some Bi and $AgBiS_2$ impurity are detected (Fig. 6(c) and (d)) Therefore, we can know that L-cystine plays an important role in the synthesis of flower-like $AgBiS_2$ crystals in the current system.

The room temperature photoluminescence (PL) spectra under the excited wavelength of 200 nm of the as-prepared $AgBiS_2$ flower-like obtain under 200 °C for 12 h was shown in Fig. 7. Besides the peak located at about 465 nm (2.67 eV), some shoulders can be also observed. The emission peak was caused by the recombination of electrons and electron holes in trapped surface states in the forbidden region, called energy band gap. But for the shoulders, they were caused by the shallow level of donors and acceptors between the valence and conduction bands [12,13].

4. Conclusions

A mild biomolecule-assisted route was proposed for the synthesis of flower-like $AgBiS_2$ using L-cystine as the sulfur source and complexing agent. In this process, the formation of metal–biomolecule complexes ($[Ag(L\text{-cystine})_n]^+$ and $[Bi(L\text{-cystine})_n]^{3+}$) and solvothermal decomposition and sulfidation are attributed to the formation of flower-like $AgBiS_2$. The X-ray diffraction and the X-ray photoelectron spectra indicated the formation of pure cubic phase $AgBiS_2$. The FESEM and the TEM images showed flower-like $AgBiS_2$ crystals with an average diameter of about 5 μm. A possible formation mechanism for flower-like $AgBiS_2$ was also discussed. The photoluminescence (PL) emission of the product produced at 200 °C for 12 h was detected at the wavelength of 465 nm (2.67 eV).

Acknowledgements

Financial support from the National Science Foundation of China (Grant Nos. 50772075 and 50972107) is gratefully acknowledged. We thank Yunhui He from Fuzhou University for obtaining the XPS patterns, and Prof. Huanming Lu from Ningbo Institute of Material Technology and Engineering of the Chinese Academy of Sciences for taking the TEM images.

References

[1] F.J. Disalvo, Science 247 (1991) 649–655.
[2] N.K. Allouche, N. Jebbari, C. Guasch, N.K. Turki, J. Alloys Compd. 501 (2010) 85–88.
[3] W.S. Sheldrick, M. Wachhold, Angew. Chem. Int. Ed. Engl. 36 (1997) 206–224.
[4] S.A. Aliev, S.S. Raginov, Neorg. Mater. 28 (1992) 329–334.
[5] M. Lei, P.G. Li, W.H. Tang, J. Alloys Compd. 509 (2011) 5020–5022.
[6] D. Chen, G.Z. Shen, K.B. Tang, X. Jiang, L.Y. Huang, Y. Jin, Y.T. Qian, Inorg. Chem. Commun. 6 (2003) 710–712.
[7] J.Q. Wang, X.K. Yang, W.B. Hu, B. Li, J.M. Yan, J.J. Hu, Chem. Commun. 46 (2007) 4931–4933.
[8] G.Z. Shen, D. Chen, K.B. Tang, Y.T. Qian, J. Cryst. Growth 252 (2003) 199–201.
[9] P.K. Nair, L. Huang, M.T.S. Nair, H. Hu, E.A. Meyers, R.A. Zingaro, J. Mater. Res. 12 (1997) 651–656.
[10] J. Zhou, G.Q. Bian, Q.Y. Zhu, Y. Zhang, C.Y. Li, J. Dai, J. Solid State Chem. 182 (2009) 259–264.
[11] G.Z. Shen, D. Chen, K.B. Tang, Y.T. Qian, J. Cryst. Growth 257 (2003) 293–296.
[12] T. Thongtem, J. Jaroenchaichana, S. Thongtem, Mater. Lett. 63 (2009) 2163–2166.
[13] T. Thongtem, N. Tipcompor, S. Thongtem, Mater. Lett. 64 (2010) 755–758.
[14] B. Xie, S.W. Yuan, Y. Jiang, J. Lu, Q. Li, Y. Wu, W.C. Yu, H.B. Zhang, Y.T. Qian, Chem. Lett. 31 (2002) 612–613.
[15] B. Pejova, I. Grozdanov, D. Nesheva, A. Petrova, Chem. Mater. 20 (2008) 2551–2565.
[16] J.Q. Jiao, X. Liu, W. Gao, C.W. Wang, H.J. Feng, X.L. Zhao, L.P. Chen, Solid State Sci. 11 (2009) 976–981.
[17] Q. Lu, Y.F. Gao, S. Komarneni, J. Am. Chem. Soc. 126 (2004) 54–55.
[18] X. Wu, K.W. Li, H. Wang, J. Alloys Compd. 487 (2009) 537–544.
[19] K.T. Nam, D.W. Kim, P.J. Yoo, C.Y. Chiang, N. Meethong, P.T. Hammond, Y.M. Chiang, A.M. Belcher, Science 312 (2006) 885–888.
[20] X.F. Yang, X.T. Dong, J.X. Wang, G.X. Liu, J. Alloys Compd. 487 (2009) 298–303.
[21] S.Z. Liu, S.L. Xiong, K.Y. Bao, J. Cao, Y.T. Qian, J. Phys. Chem. C 113 (2009) 13002–13007.
[22] J.H. Jiang, R.L. Yu, R. Yi, W.Q. Qin, G.Z. Qiu, X.H. Liu, J. Alloys Compd. 493 (2010) 529–534.
[23] J.H. Jiang, R.N. Yu, J.Y. Zhu, R. Yi, G.Z. Qiu, Y.H. He, X.H. Liu, Mater. Chem. Phys. 115 (2009) 502–506.
[24] J.S. Zhong, J. Hu, W. Cai, F. Yang, L.J. Liu, H.T. Liu, X.Y. Yang, X.J. Liang, W.D. Xiang, J. Alloys Compd. 501 (2010) L15–L19.
[25] J.S. Zhong, W.D. Xiang, H.D. Jin, W. Cai, L.J. Liu, X.Y. Yang, X.J. Liang, H.T. Liu, Mater. Lett. 64 (2010) 1499–1502.
[26] M.L. Pang, J.Y. Hu, H.C. Zeng, Synthesis, J. Am. Chem. Soc. 132 (2010) 10771–10785.
[27] M.S. Niasari, M. Bazarganipour, F. Davar, J. Alloys Compd. 489 (2010) 530–534.
[28] J.W. Thomson, L. Cademartiri, M. MacDonald, S. Petrov, G. Calestani, P. Zhang, G.A. Ozin, J. Am. Chem. Soc. 132 (2010) 9058–9068.
[29] V.V. Atuchin, L.I. Isaenko, V.G. Kesler, S.I. Lobanov, J. Alloys Compd. 497 (2010) 244–248.
[30] J.H. Kim, H. Park, C.H. Hsu, J. Xu, J. Phys. Chem. C 114 (2010) 9634–9639.
[31] J.H. Xiang, H.Q. Cao, Q.Z. Wu, S.C. Zhang, X.R. Zhang, A.A.R. Watt, J. Phys. Chem. C 112 (2008) 3580–3584.
[32] N. Burford, M.D. Eelman, W.G. LeBlanc, T.S. Cameron, K.N. Robertson, Chem. Commun. 3 (2004) 332–333.
[33] X.Y. Chen, X.F. Zhang, Z.H. Wang, J.X. Wan, Y.T. Qian, Mater. Chem. Phys. 98 (2006) 419–421.
[34] B.X. Li, Y. Xie, Y. Xue, J. Phys. Chem. C 111 (2007) 12181–12187.
[35] W. Chen, Z.G. Wang, Z.J. Lin, L.Y. Lin, J. Appl. Phys. 82 (1997) 3111–3115.